




Micro-Doppler-Based UAVs Classification Using Improved Quantum Genetic SVM

1st Urszula Libal 

*Faculty of Electronics, Photonics and Microsystems
Wroclaw University of Science and Technology
Wroclaw, Poland*

2nd Agnieszka Wielgus 

*Faculty of Electronics, Photonics and Microsystems
Wroclaw University of Science and Technology
Wroclaw, Poland*

3rd Dawid Podgórski 

*Faculty of Electronics, Photonics and Microsystems
Wroclaw University of Science and Technology
Wroclaw, Poland*

4th Karol Abratkiewicz 

*Institute of Electronic Systems
Warsaw University of Technology
Warsaw, Poland*

Abstract—This paper addresses the critical challenge of classifying small aerial targets, particularly unmanned aerial vehicles (UAVs), using micro-Doppler radar signatures. We present a novel, computationally efficient feature extraction method that transforms raw radar data into a 108-dimensional spectral feature vector, capturing both dominant frequency components and time-frequency energy distribution. This approach significantly reduces data complexity, enabling the use of simpler, yet highly effective, classifiers. We employ an Improved Quantum Genetic Algorithm (IQGA) to optimize the hyperparameters of a Support Vector Machine (SVM) with a Radial Basis Function (RBF) kernel. The IQGA-SVM achieved a classification accuracy of 99.59% on the DIAT-uSAT dataset, outperforming standard SVMs, Multilayer Perceptrons (MLPs), and deep learning models such as VGG16, VGG19, and DIAT-RadSATNet. Our results demonstrate that meticulously engineered spectral features provide a more discriminative representation than raw spectrogram data, allowing simpler classifiers to achieve superior performance with significantly lower computational overhead. This study highlights the efficacy of feature engineering and quantum-inspired optimization for robust and efficient UAV classification, offering a practical solution for airspace security.

Index Terms—Micro-Doppler, UAV type recognition, quantum genetic algorithm, feature extraction, radar signal processing

I. INTRODUCTION

The rapid increase in low-altitude unmanned aerial vehicles (UAVs) poses a significant airspace security challenge. Their small size and low detectability necessitate specialized detection technologies to counter potential illicit activities and protect critical infrastructure [1], [2]. Micro-Doppler radar signatures play an important role in UAV type recognition.

Harmanny et al. in [3] stated that spectrograms and cepstograms can be used to extract key features of low-altitude slow-moving small targets versus bio-life. The variance on the extracted periodicity was used as a feature to distinguish between single, stable rotor/propeller carrying targets and multicopters. In [4], authors extracted 13 features from intrinsic mode functions, which, together with the TERRM classifier,

were observed to possess discriminative information for UAVs classification (non-UAV vs. fixed-wing UAV vs. rotary-wing UAV). In [5], the authors proposed two novel features: the number of P -crossing and the correlation of amplitude peaks and used them to train and evaluate a binary-category classifier.

For spectrograms of micro-Doppler signatures, convolutional neural networks (CNNs) present a logical analytical framework. This very popular approach has been explored in numerous works. In [6], the authors proposed a novel image representation generated through the fusion of the micro-Doppler signature and the cadence-velocity diagram, termed the merged Doppler image. The GoogLeNet CNN architecture was employed to classify these generated image data. Similarly, classification based on a micro-Doppler spectrogram images, employing GoogLeNet CNN architecture, with the objective of distinguishing between drone and bird classes, was proposed in [7]. The problem of the classification between flying birds and rotary-wing drones using CNN was considered also in [8]. The authors of [9] classified three drone model types utilizing low-uncertainty micro-Doppler signature images and ultra-lightweight CNN. To address aerial target recognition with limited radar data, a robust relation network (RRN-ATR-Net), a specialized CNN architecture designed for few-shot learning, was implemented in [10]. In [11], the authors utilized their proprietary DIAT- μ SAT dataset, comprising micro-Doppler signature images of five distinct small aerial targets. They proposed a transfer learning-based deep CNN approach, employing VGG16 and VGG19 as feature extractors, to classify low radar cross-section aerial targets. Subsequently, using the same dataset, [12] introduced a novel model DIAT-RadSATNet. This model was designed according to a set of novel principles and optimized across multiple factors, including layer configuration, parameter count, floating-point operations (FLOPs), block structure, filter dimensions, memory footprint, parallel path count, and classification accuracy. The model's architecture was refined through a series of comprehensive ablation studies.

While spectrogram-based CNNs represent a widely adopted

This activity was sponsored by the NATO Science & Technology Organization Office of the Chief Scientist under grant id. OCSWP30008.

approach, other techniques, such as a long short-term memory (LSTM) neural network [13] applied to micro-Doppler signature data for the purposes of detecting and classifying small UAVs, have been also investigated.

This study introduces computationally efficient and position-invariant features for UAV classification, effectively mitigating range dependency in radar cross-section measurements. High classification accuracy is achieved using a kernel SVM classifier whose parameters were optimized with an Improved Quantum Genetic Algorithm (IQGA).

II. KERNEL SUPPORT VECTOR MACHINES

The fundamental concept behind Support Vector Machines (SVMs) [14] involves identifying the optimal hyperplane

$$w^T \cdot x + b = 0, \quad (1)$$

which separates data points: $\{(x_1, y_1), (x_2, y_2), \dots, (x_n, y_n)\}$, where x_i are feature vectors belonging to classes y_i . The determination of this hyperplane is achieved by maximizing the margin, which quantifies the distance between the hyperplane and the nearest data points of each class, referred to as support vectors. Among the various kernel functions, the Radial Basis Function (RBF) [15]:

$$K(x_i, x_j) = \exp(-\gamma \|x_i - x_j\|^2) \quad (2)$$

is widely adopted for modeling complex, non-linear decision boundaries. The hyperparameter γ controls the width of the Gaussian function, thereby influencing the smoothness of the decision boundary.

According to Karush-Kuhn-Tucker (KKT) conditions, the determination of the hyperplane weight vector can be solved by a dual optimization problem involving dual variables a_i :

$$\begin{cases} \text{maximize:} & \sum_{i=1}^n a_i - \frac{1}{2} \sum_{i=1}^n \sum_{j=1}^n a_i a_j y_i y_j K(x_i, x_j) \\ \text{subject to:} & \sum_{i=1}^n a_i y_i = 0 \text{ and } C \geq a_i \geq 0 \\ & \text{for } i = 1, \dots, n. \end{cases} \quad (3)$$

The regularization parameter C regulates the balance between model complexity and training error, significantly impacting the SVMs ability to generalize.

III. IMPROVED QUANTUM GENETIC ALGORITHM

To find optimal parameters C and γ of the SVM kernel, an Improved Quantum Genetic Algorithm (IQGA) [16] was applied. Since IQGA is based on principles of quantum computing, instead of a single gene, there is a qubit represented by $[\alpha, \beta]^T$, $|\alpha|^2 + |\beta|^2 = 1$ and each individual is represented as a qubits' vector:

$$\begin{bmatrix} \alpha_1 & \alpha_2 & \dots & \alpha_m \\ \beta_1 & \beta_2 & \dots & \beta_m \end{bmatrix}. \quad (4)$$

The chromosomes code SVM parameters: γ and C . With each individual, a fitness function $f(p_i)$ is connected. The current quantum state $|\psi\rangle$ is given as $|\psi\rangle = \alpha|0\rangle + \beta|1\rangle$, where α is a probability the quantum state collapses into the '0' state,

and β is a probability the quantum state collapses into the '1' state.

In quantum genetic algorithms, the individuals evolve according to a quantum rotation gate:

$$R(\Delta\theta) = \begin{bmatrix} \cos(\Delta\theta_i) & -\sin(\Delta\theta_i) \\ \sin(\Delta\theta_i) & \cos(\Delta\theta_i) \end{bmatrix}. \quad (5)$$

Next, the chromosomes are updated:

$$|\psi\rangle' = R(\Delta\theta) \times |\psi\rangle = \begin{bmatrix} \cos(\Delta\theta_i) & -\sin(\Delta\theta_i) \\ \sin(\Delta\theta_i) & \cos(\Delta\theta_i) \end{bmatrix} \begin{bmatrix} \alpha \\ \beta \end{bmatrix} = \begin{bmatrix} \alpha' \\ \beta' \end{bmatrix}. \quad (6)$$

$|\psi\rangle'$ is a new quantum state, and the direction and value of $\Delta\theta$ are set by strategy adjusting presented in Table I. Let $q(p_i)$ and $q(b_i)$ denote the current qubit state of individual p_i and the current best individual, respectively. The fitness of individual p_i is given by $f(p_i)$ with f_{opt} representing the fitness of the best individual. The rotation angle applied to $q(p_i)$ is represented by $\Delta\theta_i$. The following four columns define the rotation direction: where +1 indicates counter-clockwise, -1 indicates clockwise, and ± 1 signifies a randomly selected direction.

TABLE I
LOOKUP TABLE OF ROTATION SCHEME

$q(p_i)$	$q(b_i)$	$f(p_i) \geq f_{\text{opt}}$	$\Delta\theta_i$	$\alpha_i \beta_i > 0$	$\alpha_i \beta_i < 0$	α_i	β_i
0	0	False	0	0	0	0	0
0	0	True	0	0	0	0	0
0	1	False	σ	+1	-1	0	± 1
0	1	True	σ	-1	+1	± 1	0
1	0	False	σ	-1	+1	± 1	0
1	0	True	σ	+1	-1	0	± 1
1	1	False	0	0	0	0	0
1	1	True	0	0	0	0	0

The population is split into subpopulations with equal numbers of individuals, and with a given number of iterations, randomly selected individuals are exchanged through crossover operations. To modulate the search process (diversification and intensification) the rotation angle is iteratively reduced. Let $\Delta\theta_i$ represent the rotation angle at iteration i , then:

$$\Delta\theta_i = k(\theta_{\text{max}} - \theta_{\text{min}}) + \theta_{\text{min}} \quad (7)$$

and

$$k = \arcsin \frac{f_{\text{opt}} - f_c}{f_{\text{opt}}}, \quad (8)$$

where f_{opt} is the optimal individual fitness and f_c is the current individual fitness, θ_{max} and θ_{min} are the maximum and minimum angles of rotation. To protect from premature convergence, if the qubit parameters α and β approach values of 0 or 1 within a tolerance of ϵ , they are adjusted accordingly at the quantum convergence gate H_ϵ [17]:

$$[\alpha'_i \beta'_i] = H_\epsilon(\alpha_i, \beta_i, \Delta\theta_i). \quad (9)$$

For $[\alpha''_i \beta''_i]^T = R(\Delta\theta_i)[\alpha'_i \beta'_i]^T$, we consider the cases:

- if $|\alpha''_i|^2 \leq \epsilon$ and $|\beta''_i|^2 \geq 1 - \epsilon$, then $[\alpha'_i \beta'_i]^T = [\sqrt{\epsilon} \sqrt{1 - \epsilon}]^T$,
- if $|\alpha''_i|^2 \geq 1 - \epsilon$ and $|\beta''_i|^2 \leq \epsilon$, then $[\alpha'_i \beta'_i]^T = [\sqrt{1 - \epsilon} \sqrt{\epsilon}]^T$,

- else $[\alpha'_i \beta'_i]^T = [\alpha''_i \beta''_i]^T$.

The main steps of IQGA are as follows:

- 1) Initialization: determine C and γ range (C_r and γ_r , respectively), population size n , iteration number $iter_{max}$, set $iter = 0$, $C_{opt} = 1$, $\gamma_{opt} = 0$, $f_{opt} = 0$, calculate number of necessary qubits to code C and γ , set number of subpopulations N_s , determine iteration interval for crossover cr_{iter} and θ_{min} and θ_{max} values.
- 2) Initialize first population: set α and β to random values in $(0, 1)$.
- 3) Divide the population into N_s subpopulations.
- 4) Evaluation: train SVM model and calculate accuracy on the validation set.
- 5) Record the best individual and its fitness f_{opt} .
- 6) Evolution: for each subpopulation, update the individuals by performing a dynamic rotation angle quantum gate operation, use quantum convergence gate H_ϵ , set $iter = iter + 1$.
- 7) Apply mutation.
- 8) If $iter$ is equal to cr_{iter} , do crossover.
- 9) If the stop condition is not met, go to step 3. Else, return the best values of C_{opt} and γ_{opt} .

IV. DATASET

The dataset used to evaluate the proposed method, known as DIAT- μ SAT, originates from [11], [12]. This dataset comprises 4849 UAV signals recorded using a continuous-wave radar operating in the X band. The authors recorded five different targets and categorized them into six classes: two-blade and three-blade rotors (each with short and long blades), quadcopters, bionic birds, and a mixed class combining a two-blade rotor and a bionic bird.

Each target was captured in 3-second-long recordings, preserving the echo of the target while maintaining a constant position during flight. A detailed description of the database is provided in [11], [12]; however, the key parameters relevant to this work are summarized in Table II. Notably, the revolutions per minute (RPM) play a crucial role in further analysis.

TABLE II
CLASSES OF SMALL AERIAL TARGETS IN DIAT- μ SAT DATASET

Class name	Approx. speed of operation
Two-blade rotor	300 – 1740 RPM
Three short-blade rotor	250 – 1410 RPM
Three long-blade rotor	200 – 1050 RPM
Quadcopter	2000 – 7000 RPM
Bionic bird	2 – 4 flaps/s
Two-blade rotor & Bionic bird	300 – 1530 RPM & 2 – 4 flaps/s

In the original dataset, the authors processed the signals into spectrograms, with each signal first undergoing low-pass filtering (0 – 2 kHz) to remove high-frequency artifacts. The resulting spectrograms amounted to a total data volume of 1052.9 MB. In this work, we significantly reduced the data size by extracting 4849 compact feature vectors (of only 108 features), making the dataset more lightweight (3.99 MB) and efficient for further processing.

V. FEATURE EXTRACTION

The feature extraction can be summarized as follows. The signal undergoes preprocessing, where it is centered by removing the mean, downsampled to reduce data size, and filtered using a high-pass (above 5 Hz) filter to eliminate low-frequency noise, antenna leakage, and clutter.

Following preprocessing, frequency-domain analysis is performed by computing the Fast Fourier Transform (FFT) of the filtered signal. From the normalized amplitude spectrum, the five dominant frequency peaks were identified. These peaks, visualized for all categories of analyzed UAVs in the left column of Fig. 1, represent critical spectral components and constitute the first portion of the extracted feature vector. A search for frequency peaks was conducted within the 0–50 Hz range for all classes. While quadcopters exhibit approximate operational speeds ranging from 2000 to 7000 RPM (Table II), which theoretically translates to frequency peaks within the 33–116 Hz range, the requirement for a unified feature extraction and classification pipeline across all aerial target classes was paramount. This unification, essential for the automatic recognition of UAV categories, dictated the application of the consistent 0–50 Hz search range to all input signatures.

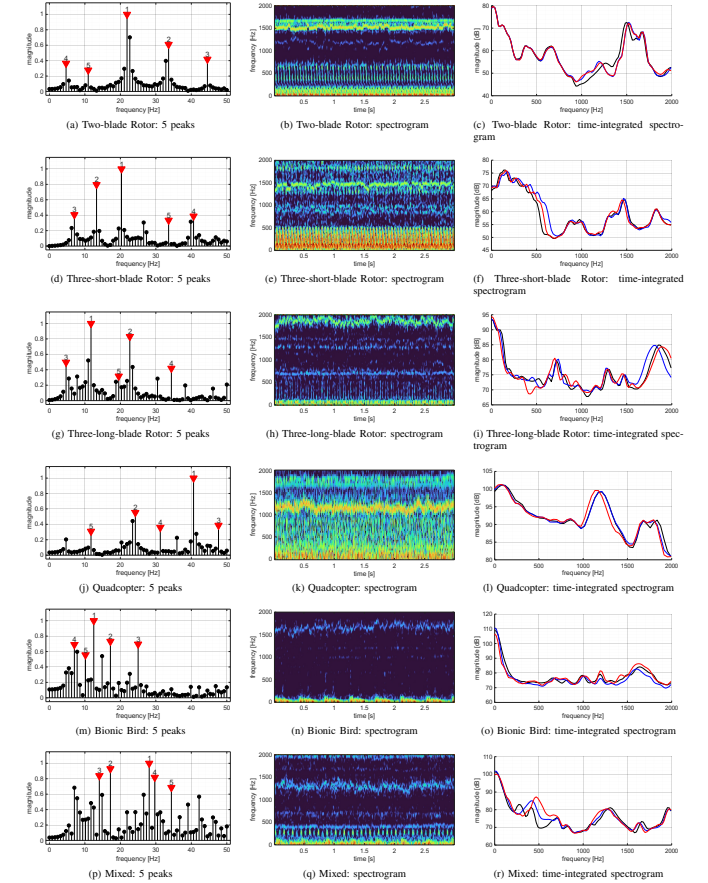


Fig. 1. Signal preprocessing and feature extraction: five dominant frequency peaks (5 features), spectrograms, time-integrated spectrograms (103 features).

To incorporate time-frequency information, the spectrogram of the original, full-band signal $x[n]$ is computed. The spec-

rogram $S[t, f]$ represents the squared magnitude of the Short-Time Fourier Transform (STFT):

$$S[t, f] = |STFT(x[n])|^2. \quad (10)$$

This captures the frequency evolution over time. A frequency range of 0 to 2000 Hz, shown in spectrograms presented in the central column of Fig. 1, is selected to focus on relevant spectral components.

The time-integrated magnitude of the spectrogram within this range is then calculated as:

$$I[f] = \sum_t S[t, f] \text{ for } 0 \leq f \leq 2000 \text{ Hz}. \quad (11)$$

This time-integrated magnitude $I[f]$ provides a representation of the spectral energy distribution over the selected frequency range and is presented in the right column of Fig. 1.

Subsequently, the five extracted dominant frequency peaks and the 103 elements of the time-integrated spectrogram magnitude $I[f]$ are concatenated, resulting in a 108-dimensional feature vector¹. This representation of 4849 signals compresses the dataset into a 3.99 MB MAT data file. This vector serves as the input for the subsequent automatic classification of small aerial targets. The combined feature vector effectively encapsulates both the dominant frequency components and the time-frequency energy distribution of the signal, providing a comprehensive representation suitable for classification.

VI. NUMERICAL EXPERIMENT AND DISCUSSION

The IQGA-SVM was trained and optimized exclusively on 90% of DIAT- μ SAT dataset, preserving the data division applied in [11]. The training set consisted of 80% and the validation set of 10% of randomly chosen data from the mentioned 90%. The remaining 10% was used for testing. We examined the algorithm for the following sets of parameters: population size $P = 40$, number of subpopulation $N_s = 4$, crossover threshold $cr_{iter} = 10$, as a mutation we switched values in a random qubit. The experiments were held for the following θ range: $\theta_{max} = \pi/2$ and $\theta_{min} = \pi/5$ and $\epsilon = 0.0001$. The values of C and γ are from the predefined neighborhood $C \in [0.4, 4]$, $\gamma \in [10^{-7}, 1.0]$. The resulting confusion matrix for the IQGA-SVM is shown in Fig. 2.

For comparative analysis, the DIAT- μ SAT dataset was also classified using standard SVM and MLP. The classification accuracies are presented in Table III. The results of classifying small aerial targets from the DIAT- μ SAT dataset demonstrate a clear advantage of employing engineered spectral features (according to method proposed in Section V) over direct processing of colorful spectrograms (as in [11] and [12]). Our feature extraction methodology, which reduced the complex signal information into a concise 108-dimensional feature vector, proved highly effective across various classifiers. Notably, the IQGA-SVM, employing an RBF kernel and optimized parameters C_{opt} and γ_{opt} , achieved a remarkable accuracy of 99.59%. This significantly surpasses the performance of all

Two-blade Rotor	80	0	0	0	0	0
Three-short-blade Rotor	1	79	0	0	0	0
Three-long-blade Rotor	0	0	80	0	0	0
Quadcopter	0	0	0	83	0	0
Bionic Bird	0	0	0	0	80	0
Mixed	0	0	1	0	0	81
True labels	Two-blade Rotor	Three-short-blade Rotor	Three-long-blade Rotor	Quadcopter	Bionic Bird	Mixed
	Predicted labels					

Fig. 2. Confusion matrix for IQGA-SVM, trained on 80%, validated on 10% and tested on 10% of DIAT- μ SAT dataset.

other models, including deep learning architectures, underscoring the power of well-crafted features in capturing essential discriminative information. On a computer with AMD Ryzen Threadripper PRO 5955WX (16-cores, 4 GHz, 128 GB RAM), the average processing time for a single radar signature was 150 ms in MATLAB, which is short for processing a 3-second recording. Furthermore, UAV type recognition in Python was completed in under 97 μ s. This rapid computational capability allows the trained IQGA-SVM to be effectively implemented in real-time aerial target recognition systems.

The effectiveness of our feature set is further evidenced by the strong performance of simpler classifiers. Standard SVM with an RBF kernel, despite not benefiting from the IQGA optimization, still achieved a respectable accuracy of 95.88%. This indicates that the extracted features are inherently robust and informative. Moreover, the MLP models showcased a consistent improvement in accuracy with increasing network depth, culminating in a 98.97% accuracy for the 3-layer MLP. This trend highlights the ability of these features to facilitate training even in relatively straightforward network structures.

In stark contrast, the deep learning models: VGG16 and VGG19 from [11], and DIAT-RadSATNet from [12], which directly processed colorful spectrograms of size $[224 \times 224 \times 3]$, exhibited lower overall performance. While these models achieved accuracies ranging from 95% to 97.3%, they required significantly larger parameter counts and more complex architectures. VGG16 and VGG19, in particular, utilized over 138 million and 143 million parameters, respectively, compared to the IQGA-SVM. Even DIAT-RadSATNet model, with its more efficient design, still employed 0.45 million parameters. This discrepancy in parameter counts highlights the computational efficiency of our feature extraction approach, which allows for high accuracy with significantly reduced model complexity.

The results strongly suggest that the detailed spectral information encapsulated within our 108 features provides a more discriminative representation of the targets compared to the raw spectrogram data. By focusing on key spectral components and their temporal evolution, we effectively condensed the essential information, enabling simpler classifiers to outperform complex deep learning models. This demonstrates the potential of signal processing and feature engineering to streamline classification tasks, especially in scenarios where

¹The MATLAB function is publicly available at: <https://github.com/kabratkiewicz/Micro-Doppler-Feature-Extraction>

TABLE III
CLASSIFICATION ACCURACY TO 6 CLASSES OF SMALL AERIAL TARGETS FROM DIAT- μ SAT DATASET

Classifier	Kernel Params.	No. Features	Accuracy [%]	No. Classifier Params.
IQGA-SVM (kernel = RBF)	$\begin{cases} C_{\text{opt}}=3.475 \\ \gamma_{\text{opt}}=3.845 \times 10^{-4} \end{cases}$	108	99.59	2 + No. support vectors
SVM (kernel = RBF)	$C=1, \gamma=1/108$	108	95.88	2 + No. support vectors
SVM (kernel = Linear)	$C=1$	108	93.40	1+15 \times 109
MLP (1 layer: 100)	–	108	97.53	11,506
MLP (2 layers: 100-100)	–	108	98.14	21,606
MLP (3 layers: 100-100-100)	–	108	98.97	31,706
VGG16 [11] (16 layers)	–	224 \times 224 \times 3	95.00	138M
VGG19 [11] (19 layers)	–	224 \times 224 \times 3	97.00	143M
DIAT-RadSATNet [12] (4 RsE blocks, 40 layers)	–	224 \times 224 \times 3	97.30	0.45M

computational resources are limited or real-time processing is crucial. Furthermore, the ability to achieve high accuracy with a small number of features opens the door for more efficient and interpretable classification systems.

VII. CONCLUSION

The results demonstrate the effectiveness of our feature extraction and signal preprocessing. By distilling the raw signal into a concise 108-dimensional feature vector, we enabled simpler classifiers, specifically the SVM and deeper MLP architectures, to achieve exceptional classification accuracy. Notably, the IQGA-SVM, with its optimized parameters, achieved accuracy of 99.59% and outperformed all other models, including complex deep learning networks. This highlights the power of well-engineered features in capturing the essential information required for accurate classification. In contrast, while deep learning models like VGG16, VGG19, and DIAT-RadSATNet achieved respectable results, they relied on significantly larger parameter counts and more complex architectures to process raw spectrograms. Our approach underscores that sophisticated feature extraction can streamline the classification process, allowing simpler and more efficient classifiers to deliver superior performance compared to resource-intensive deep learning models. This signifies a substantial advantage in applications where computational efficiency and model simplicity are paramount.

ACKNOWLEDGMENT

The authors would like to thank the creators of DIAT- μ SAT dataset [11]: H.C. Kumawat, M. Chakraborty, A.A.B. Raj and S.V. Dhavale, for access to their database comprising continuous-wave X band radar signatures of aerial targets.

REFERENCES

- [1] A. Yasmeen and O. Daescu, "Recent Research Progress on Ground-to-Air Vision-Based Anti-UAV Detection and Tracking Methodologies: A Review," *Drones* (2504-446X), vol. 9, no. 1, 2025.
- [2] K. Bremnes, R. Moen, S. R. Yeduri, R. R. Yakkati, and L. R. Cenkeramaddi, "Classification of UAVs utilizing fixed boundary empirical wavelet sub-bands of RF fingerprints and deep convolutional neural network," *IEEE Sensors Journal*, vol. 22, no. 21, pp. 21 248–21 256, 2022.
- [3] R. I. Harmanny, J. J. de Wit, and G. Premel-Cabic, "Radar micro-Doppler mini-UAV classification using spectrograms and cepstrograms," *International Journal of Microwave and Wireless Technologies*, vol. 7, no. 3-4, pp. 469–477, 2015.
- [4] B.-S. Oh, X. Guo, and Z. Lin, "A UAV classification system based on FMCW radar micro-Doppler signature analysis," *Expert Systems with Applications*, vol. 132, pp. 239–255, 2019.
- [5] B.-S. Oh and Z. Lin, "Extraction of Global and Local Micro-Doppler Signature Features From FMCW Radar Returns for UAV Detection," *IEEE Transactions on Aerospace and Electronic Systems*, vol. 57, no. 2, pp. 1351–1360, 2021.
- [6] B. K. Kim, H.-S. Kang, and S.-O. Park, "Drone classification using convolutional neural networks with merged Doppler images," *IEEE Geoscience and Remote Sensing Letters*, vol. 14, no. 1, pp. 38–42, 2016.
- [7] S. Rahman and D. A. Robertson, "Classification of drones and birds using convolutional neural networks applied to radar micro-Doppler spectrogram images," *IET Radar, Sonar & Navigation*, vol. 14, no. 5, pp. 653–661, 2020.
- [8] X. Chen, H. Zhang, J. Song, J. Guan, J. Li, and Z. He, "Micro-motion classification of flying bird and rotor drones via data augmentation and modified multi-scale CNN," *Remote Sensing*, vol. 14, no. 5, p. 1107, 2022.
- [9] J. Park and J.-S. Park, "Classification of Small Drones Using Low-Uncertainty Micro-Doppler Signature Images and Ultra-Lightweight Convolutional Neural Network," *IEEE Transactions on Image Processing*, vol. 33, pp. 2979–2994, 2024.
- [10] Z. Wu and Z. Liu, "RRN-ATR-Net: A Robust Relation Network for Aerial Targets Recognition Based on Two-Stream Micro-Doppler Signatures Fusion," *IEEE Transactions on Instrumentation and Measurement*, vol. 74, pp. 1–12, 2025.
- [11] H. C. Kumawat, M. Chakraborty, A. A. Basil Raj, and S. V. Dhavale, "DIAT- μ SAT: Small Aerial Targets' Micro-Doppler Signatures and Their Classification Using CNN," *IEEE Geoscience and Remote Sensing Letters*, vol. 19, pp. 1–5, 2022.
- [12] H. C. Kumawat, M. Chakraborty, and A. A. B. Raj, "DIAT-RadSATNet—A Novel Lightweight DCNN Architecture for Micro-Doppler-Based Small Unmanned Aerial Vehicle (SUAV) Targets' Detection and Classification," *IEEE Transactions on Instrumentation and Measurement*, vol. 71, pp. 1–11, 2022.
- [13] Y. Sun, S. Abeywickrama, L. Jayasinghe, C. Yuen, J. Chen, and M. Zhang, "Micro-Doppler signature-based detection, classification, and localization of small UAV with long short-term memory neural network," *IEEE Transactions on Geoscience and Remote Sensing*, vol. 59, no. 8, pp. 6285–6300, 2020.
- [14] C. Cortes and V. Vapnik, "Support-Vector Networks," *Mach. Learn.*, vol. 20, no. 3, pp. 273–297, Sep. 1995.
- [15] B. Schölkopf, A. Smola, and K.-R. Müller, "Nonlinear Component Analysis as a Kernel Eigenvalue Problem," *Neural Computation*, vol. 10, no. 5, pp. 1299–1319, July 1998.
- [16] F. Wang, K. Xie, L. Han, M. Han, and Z. Wang, "Research on support vector machine optimization based on improved quantum genetic algorithm," *Quantum Information Processing*, vol. 22, no. 380, 2023.
- [17] K.-H. Han and J.-H. Kim, "Quantum-inspired evolutionary algorithms with a new termination criterion, H/sub/spl epsi//gate, and two-phase scheme," *IEEE Transactions on Evolutionary Computation*, vol. 8, no. 2, pp. 156–169, 2004.